Rev.Adv.Mater.Sci. 11 (2006) 122-129

FEATURES OF ELECTRONIC STRUCTURE FOR NANOCRYSTALLINE METAL

R.R. Mulyukov

Institute for Metals Superplasticity Problems, Russian Academy of Science, Khalturin str. 39, Ufa 450001, Russia

Received: August 16, 2005

Abstract. Investigations of nanocrystalline (NC) tungsten samples by field emission methods showed that energy-distributions of field-emitted electrons from NC tungsten differ significantly from energy-distributions of coarse-grained metal. Measurements by an electron beam retarding potential technique displayed the reduction of work function due to formation of NC structure in metal. The revealed features are explained using two phase model for NC metal.

1. INTRODUCTION

Properties of nanocrystalline (NC) materials [1-3] with a mean grain size of about 10-100 nm are essentially distinguished from those of coarse-grained ones. This difference is attributed not only to the small NC grain size but also to the changes occurring in other structure levels of a material, in particular, electron one [3]. Especially, it concerns the role of electrons belonging to the external atom shell the collectivization of which generates large bonding energy and influences properties of metals and alloys.

The results for investigations of total energy distribution of electrons and work function of NC metal are presented in this paper.

2. EXPERIMENTAL PROCEDURE

Methods of transmission electron microscopy, field ion and field electron emissions, and an electron beam retarding potential technique were used to study features of microstructure and electronic structure of the NC tungsten (purity of 99.99%). The NC structure was obtained by high plastic deformations up to the true logarithmic strain e=7 by means of torsion under quasihydrostatic pressure on a Bridgemen anvil. The microstructure of the NC sample was studied using a transmission electron microscope JEM-2000EX.

The disk nanocrystalline samples for investigations of microstructure by transmission electron microscopy and for measurements of work function were about 10 mm in diameter and 0.1-0.2 mm. Samples for investigations of the microstructure in a field-ion microscope were produced from NC tungsten in the form of point emitters with a radius of curvature, ~30-50 nm, by means of electrolytic etching. The tip was spot welded to a metal loop. The field-ion microscope was equipped with a microchannel ion-electron converter, which intensified the brightness of surface micropatterns by a factor of 104. Liquid nitrogen was used as a coolant (T=78K). Spectroscopically pure neon was used as imaging gas.

Corresponding author: R.R. Mulyukov, e-mail: radik@anrb.ru

The field emitter tips, prepared for investigations using field emission methods, had an atomically smooth surface which was close to semi-spherical. The surface was prepared in situ by field evaporation. A controlled removal of atomic layers from the sample surface was carried out until a grain boundary appeared on a field ion image.

The tip with grain boundaries at the apex was installed in a field-electron spectrometer to study features of the electronic structure of the material. Experimental studies were conducted under conditions of ultra high (<10^{-8} Pa) vacuum. The spectrometer was equipped with a field-electron microscope for continuous observation of the emission pattern and a dispersive electrostatic energy analyzer with a resolution better 30 meV [4]. The detection of the emission current at the output of the analyzer was made possible by means of a secondary electron multiplier operated in the counting regime. The selection of the probed emission direction was achieved by means of a special manipulator. The probed area on the surface (10 nm diameter) of a point was determined by the size of the hole on the screen-anode. Measurement and processing of data were controlled by means of a personal computer and a CAMAC interface system using original software. Directly before measurements, the surface of a tip was cleaned by field desorption.

For a comparative analysis, a point, after annealing in situ at a temperature of about 800 °C for 20 minutes, was investigated. Annealing was performed by means of current passing through the nickel loop supporting the W-tip.

The electron work function was determined by the electron beam retarding technique, as was demonstrated first by Anderson [5]. The measuring part of experimental installation is three-electrode electron-optical system [6]. The system consists of a thermocathode, focusing electrode, anode with a central grid hole to release a parallel beam of electrons to the retarding area prior to the sample and the sample to which the external retarding potential V_r is applied (Fig. 1). The measuring system is placed in a work chamber of a high vacuum device. Measurements were performed in vacuum ≤10^{-3} Pa. The termocathode was made from a tungsten wire. The samples for measurement were cut in the form of a disc, about 5 mm in diameter. They were cleaned electrochemically before loading to sample holder. The retarding voltage V_r was applied to the cathode unite so that the voltage V_a between the cathode and the grid remained constant. The process of measurement of retard current on the sample and

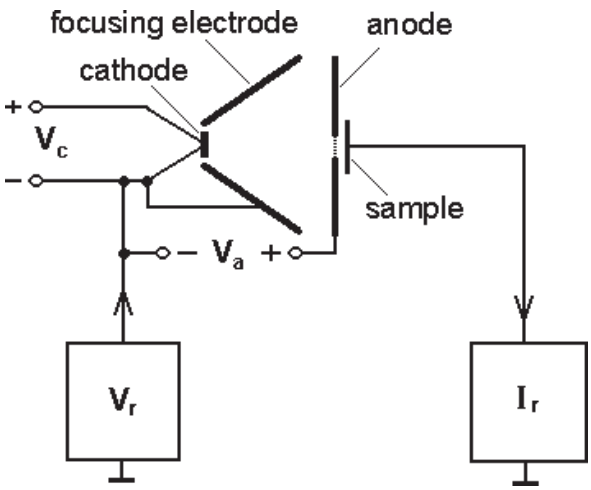

Fig. 1. Schematic diagram of the experimental arrangement.

processing of data were controlled by means a personnel computer connected with CAMAC interface using original software.

The sample - cathode system being in electric contact come to balance when their electrochemical potentials become level. At the same time there occurs the contact potential difference V_r between them which is equal to the remainder of their work function $eV_r = \phi - \phi_c$. There was performed measurement of the dependence of the current on the sample I_r (retard current) on the potential difference between the electron source and the sample V_r (retarding voltage). At first the measurement was performed on the tungsten sample with NC structure. Then this sample was annealed and the same measurement was performed on this annealed sample under similar conditions. Comparing the relative shift of curves $I_r(V_r)$ by the axis of the potential in the sample with NC structure and the annealed one the difference in the work function of the metal in two conditions $\phi_{NC} - \phi_0$. was determined.

3. RESULTS AND DISCUSSION

TEM studies have shown that severe plastic deformation resulted in NC samples (Fig. 2) with homogeneous granular structure with a mean grain size of about 100 nm [7]. A diffusion contrast of grain boundaries, and bended extinction contours within grains observed on diffraction patterns testify a non-equilibrium state of the majority of grain boundaries [3]. Annealing of the NC samples led to recovery of

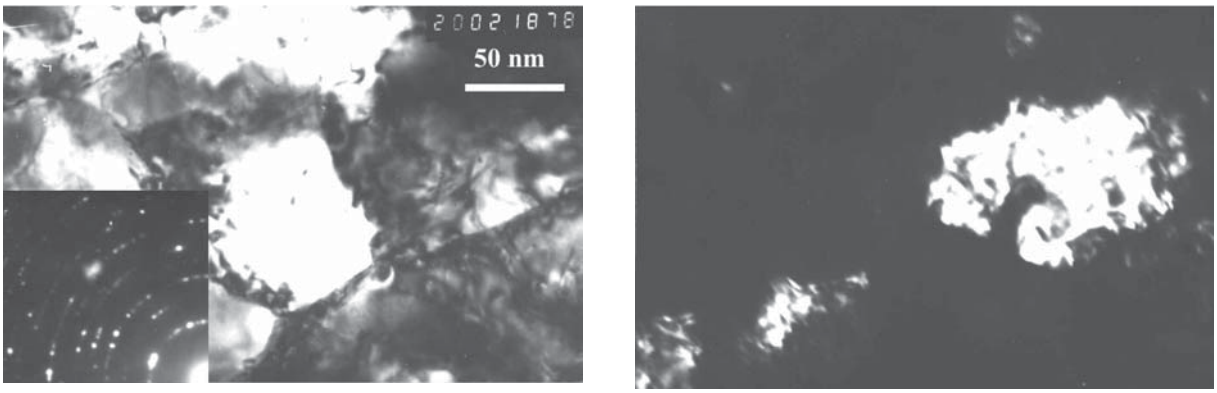

Fig. 2. Microstructure of nanocrystalline tungsten in TEM: a) light field with diffraction pattern, b) dark field.

their structure, the mean grain size increased to several micrometers. In tips of NC tungsten produced by electrolytic etching such a microstructure was preserved.

Fig. 3 shows a field ion image of the surface of NC tungsten with a grain boundary. Such a pattern of the surface was obtained by evaporating about 106 atomic layers of a (110) plane. During the removal of 43 atomic layers, the atomic structure of the grain boundaries was examined. For further field emission investigations a high angle grain boundary was selected (Fig. 3, indicated by an arrow). The analysis of the boundary structure within the tip, performed by means of controlled removal of surface atoms, has shown that its crystalline structure differs from the structure of the grain boundary of those tungsten specimen, not subjected to high plastic deformations. According to our estimations of the field ion pattern, the width of a boundary is not more than 0.6-0.8 nm. In the non-deformed tungsten this width is 0.3-0.4 nm.

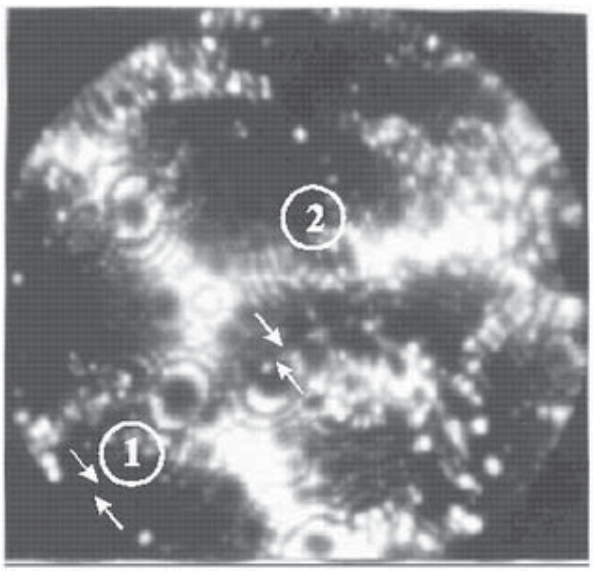

Fig. 3. Field ion image of the NC W surface (V=12.6 kV) with grain boundary (indicated by arrows). Circles 1,2 indicate portions of the surface for which total energy distributions of field-emitted electrons are given.

The atomically smooth surface of a tip, formed in a field-ion microscope, was then investigated in a field-electron spectrometer. The energy distributions of field-emitted electrons were measured for different emitting sites and the position of each site was controlled by means of the emission pattern. Though the resolution achieved by field electron microscopy is lower compared to field-ion imaging (by an order of magnitude), comparison of the two emission images allowed to identify the microstructure of areas where electron energy-distributions were taken.

Three types of total energy distributions of field-emitted electrons depending on the selected emission site on the tip were obtained [8,9]. Spectra taken from the area containing the grain boundary (Fig. 4) have an additional peak in the low energy region which or the inflection in the high energy region. An additional peak increases with increasing anode voltage (Fig. 4a) and the inflection decreases with increasing anode voltage (Fig. 4b).

In the case of areas away from the grain boundary the electron energy-distributions are similar to the classical one and expected from the Fowler-Nordheim theory (Fig. 5). However, the full-width-at-half-maximum (FWHM) of this spectrum significantly (by 0.4 eV) exceeds this parameter for the classical spectrum [10] and is 0.58-0.64 eV.

As shown before [3,11] annealing of NC samples led to recovery of their physical properties. This re-

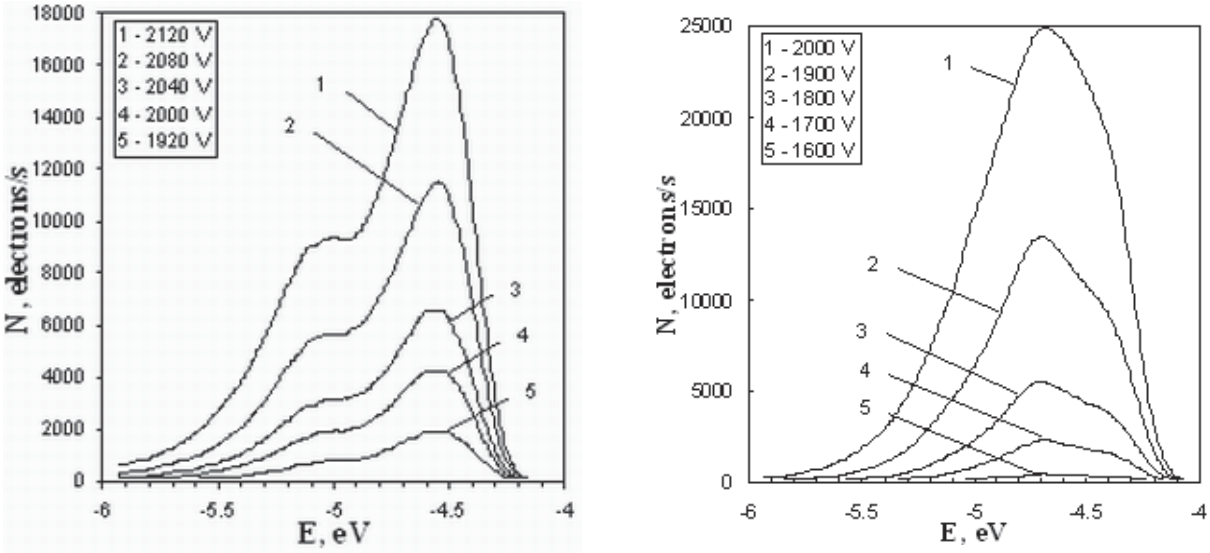

Fig. 4. Total energy distributions of field-emitted electrons from NC tungsten at different anode voltages (given in inset) obtained for different areas of surface of tip, containing a grain boundary (Fig. 3).

covery correlates with the recovery of the microstructure. In situ annealing of a tip at a temperature of about 800 °C for 20 minutes leads to a partial recovery of electron energy-distributions (Fig. 6). Only one peak was observed in the spectrum. After annealing, the FWHM decreased to 0.45-0.60 eV.

Revealed significant differences of energy characteristics of electrons emitted from NC metal and electrons emitted from coarse-grained metal can be caused by features of microstructure. In particular, we consider an elevated volume fraction of grain boundaries, being in a specific non-equilibrium state. Them effective physical width thickness significantly excesses a crystallographic width of grain boundaries and is about 10 nm [3,12]. The NC material can be presented in the form of aggregate of two phases: granular and grain boundary. The first phase has characteristics of conventional monocrystalline or coarse-grained material. The characteristics of the second phase have different fixed values. In par-

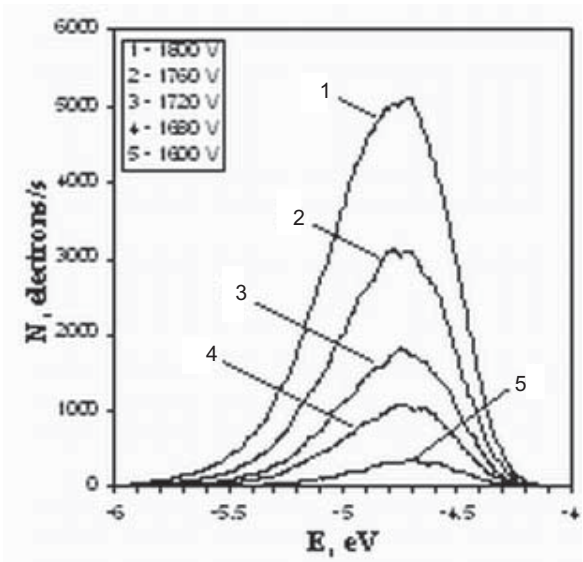

Fig. 5. Total energy distributions of field-emitted electrons from NC tungsten at different anode voltages (given in inset) obtained for area 2 (Fig. 3) away from the grain boundary.

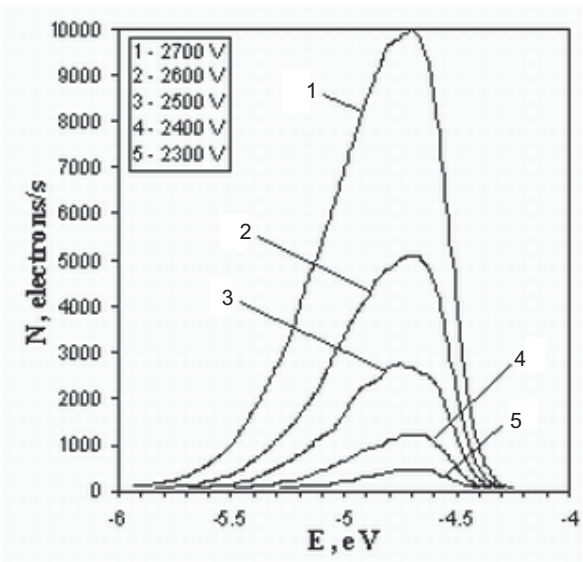

Fig. 6. Total energy distributions of field-emitted electrons at different anode voltages (given in inset) for the annealed point at 800 °C in vacuum.

ticular atoms in the second, grain boundary, phase have low (approximately on 150 °C) Debye temperature [13,14], are at dynamically excited state. Such state results in the reduction for work function. Let us consider how the reduction of work function influences on view of total energy distributions of field-emitted electron.

For interpreting the experimental data let us do the following [9,15]. Let us present the experimentally measured total energy distributions of field-emitted electrons in the form

$$N = \frac{j}{e} S f(x,y), \tag{1}$$

$$f(x,y) = \frac{(\exp(x))^y}{1+\exp(x)},$$
$$x = \frac{\varepsilon - \varepsilon_F}{kT},$$
$$y = \frac{8\pi\sqrt{2m\varphi}\,\eta\left(\sqrt{e^3 E}/\varphi\right)}{2ehE} T, \tag{2}$$

where j is the emission current density, e is the elementary charge, S is the efficient area of emission, ε_F is the Fermi's energy, k is the Boltzmann's constant, T is the Kelvin's temperature, h is the Plank's constant, m is the electron mass, φ is the emission work function, E is intensity of the electric field, $\eta\left(\sqrt{e^3 E}/\varphi\right)$ is the weakly changing function of the argument [16].

Then while analyzing emission from areas containing grain boundaries one should take into account that it comprises the emission from the grain body N_0 and from the grain boundary area N_{gb}. It is assumed that grain boundary phase has the changed work function and the Fermi's level:

$$N = N_0 + N_{gh} =$$
$$\frac{j_0}{e} S_0 f_0(x,y) + \frac{j_{gh}}{e} S_{gh} f_{gh}(x-b, cy) =$$
$$\frac{j_0}{e} S_0 \left[f_0(x,y) + a f_{gh}(x-b, cy) \right], \tag{3}$$

$$a = \frac{j_{gh} S_{gh}}{j_0 S_0},$$
$$b = \frac{\Delta\varepsilon_F}{kT},$$
$$c \approx \frac{\sqrt{\varphi_{gh}}}{\sqrt{\varphi_0}}. \tag{4}$$

For determining $\Delta\varepsilon_F = (\varepsilon_F)_{gh} - (\varepsilon_F)_0$ and $\varphi_{gh} = \varphi_0 + \Delta\varphi$ let us take the following model.

Electrons of conductivity, which can emit are in a potential pit with Coulomb interaction with ions

$$\varphi_\Pi = e^2 n^{1/3}, \tag{5}$$

φ_Π is the full work function while removing an electron, n is the concentration of electrons of conductivity or ions. The Fermi's level:

$$\varepsilon_F = \frac{h^2}{2m}\left(\frac{3}{8\pi} n\right)^{2/3}. \tag{6}$$

Emission work function

$$\varphi = \varphi_\Pi - \varepsilon_F. \tag{7}$$

We assume that the change in the value φ_Π, ε_F and φ is connected with the change in the concentration n in one of crystallographic directions. Then

$$\Delta\varphi_\Pi = \varphi_\Pi \frac{\Delta n}{n},$$
$$\Delta\varepsilon_F = \frac{2}{3}\varepsilon_F \frac{\Delta n}{n},$$
$$\Delta\varphi = \varphi + \frac{1}{3}\varepsilon_F \frac{\Delta n}{n}. \tag{8}$$

Not considering the physics of the question let us study the expression (3) at definite assumptions in respect to the values φ, ε_F, Δn.

It turned out, that the distributions (3) similar to experimental ones can be formally obtained if $\varphi - \varepsilon_F > 0$, $\Delta n < 0$, from which it results that $\Delta\varepsilon_F < 0$, $\Delta\varphi < 0$, $b < 0$, $c < 1$ (Fig. 7). It is in accord with lesser quantities of the concentrations n and of the work function from the grain boundary phase. In the case of less contribution to the emission from this phase, a=0.3, it can be obtained the distribution with an additional peak in the low energy region (Fig. 7a) by numerical modeling. When the contributions from both phases are comparable, a=0.9 – the contribution with the inflection in the high energy region (Fig. 7b).

The growth of the field corresponds to a small decrease in y, a growth of a and a more distinct growth of the factor $d = {}_0/e \cdot S_0$. Numerical modeling results that with growing the field E the left maximum becomes more distinct (Fig. 8) and the right inflection decreases. This behavior corresponds to experimental data.

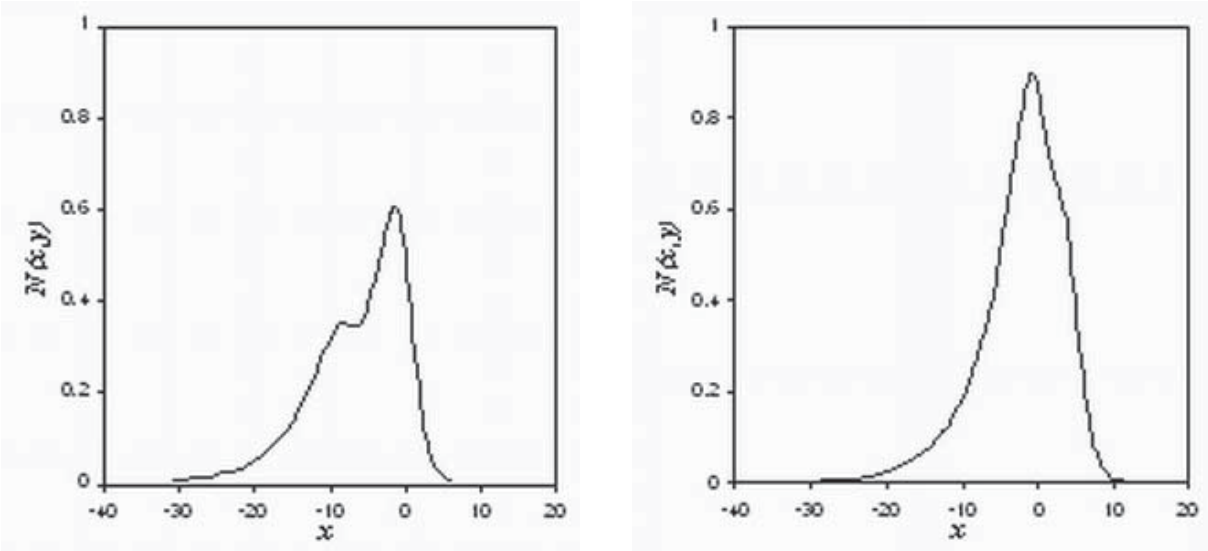

Fig. 7. Energy distribution function *N* versus *x* at *y*=0.2, *b*=-8, *c*=0.9 for a) *a*=0.3 and b) *a*=0.9.

Thus numerical modeling shows the case of decreased values of concentration *n,* Fermi's level and work function for grain boundary phase is suitable to the experiment.

Let us explain how different Fermi's levels and different work functions are reflected on total energy distributions of field-emitted electrons. Let us apply the concept from the theory of spots for work function of a non-uniform electron emitter [17]. Grain and grain boundary phases of NC metal have different Fermi's energies. Presence of electric contact with each other leads to violation of charge electric neutrality of these areas, leveling their electrochemical potentials and appearance of contact potential between spots corresponding to the exit of areas on the surface of emission. The value of contact potential is equal to the difference of work functions or the difference of Fermi's levels calculated from the energy of a rest free electron. The electric field of the contact potential or the field of spots for our case can be calculated as $E \leq 0^{-1}$ V/10^{-6} cm$\approx 10^5$ V/cm. In case of field emission the external field exceeds this value and emission occurs from separate areas with different work function that is reflected on spectra. The field of spots has a normal constituent near the metal surface and a tangential constituent at some distance. Electrons pick up transverse energy in respect to the direction of emission comparable with contact potential. This is reflected on the spectrum in the form of emission from different Fermi's levels. Decoding of spectra requires knowledge of apparatus functions of a definite device and seems to be sufficiently informational.

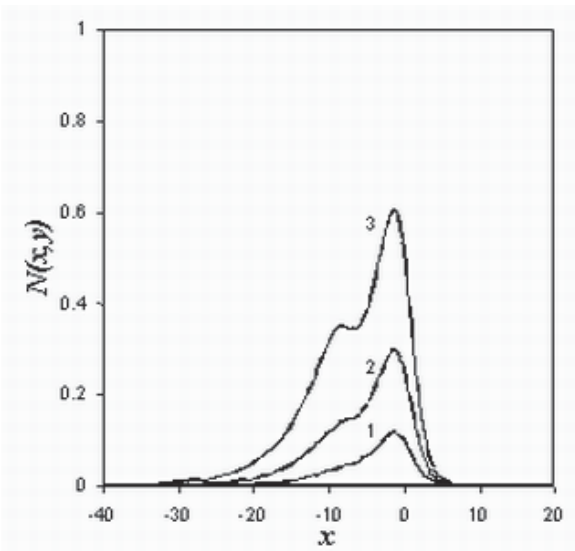

Fig. 8. Energy distribution function *N* versus *x* at 1) *y*=0.22, *a*=0.1, *d*=0.2; 2) *y*=0.21, *a*=0.2, *d*=0.5 and 3) *y*=0.20, *a*=0.3, *d*=1.

Thus reasoning from this numerical simulation it has been assumed that formation of the nanocrystalline structure in the material leads to occurrence of current paths with low work function (grain boundaries) [9,15].

The direct experimental determination of a value of work function for a NC metal is is topical both from fundamental and applied reasons. Its value is responsible for efficient operation of many types of electron sources.

The measurements of work function were made by electron beam retarding technique [6]. The results of measurement of the retard curve are shown

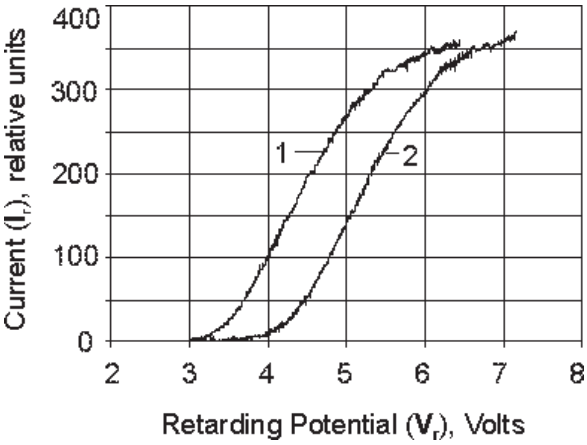

Fig. 9. Plot of retarding potential and current for nanocrystalline (1) and annealed (2) W samples.

in Fig. 9. Relative values of current are along the axis of ordinates and voltage values of V_r are along the axis of abscissa, 0 for V_r is selected conventionally. The difference in the work function for NC and annealed (coarse grained) tungsten was determined by the shift of the curves. The shift was found by the cross of approximated straight portions of lines with the abscissa axis. The curve for the NC tungsten is shifted by 0.8 V to less values of the potential as compared to the coarse-grained metal, i.e. the value of the work function for the NC metal is less by 0.8 eV.

4. CONCLUSIONS

It has been shown that energy characteristics of field-emitted electrons from NC tungsten differ from energy characteristics of coarse-grained metal. In the case of emission from the surface areas containing grain boundary the additional peak in the low energy region or the inflection in the high energy region is observed.

On the basis of the analysis performed it can be suppose that due to formation of NC structure by means of severe plastic shear straining under quasi-hydrostatic pressure paths of current with low work function (grain boundary) occur in metal.

Measurements revealed that the formation of a nanocrystalline structure results in a decrease in the electron work function of a metal. For tungsten with a grain size of about 100 nm, this decrease is equal to 0.8 V.

Presented investigation results provide finding ways for creation of highly efficient emission matrices.

ACKNOWLEDGEMNTS

The investigations were performed under the support of the Russian Foundation of Fundamental Investigations (Grant № 03-02-16560a).

REFERENCE

[1] D.I. Morokhov, L.I. Trusov and V.I. Lapovok, *Physical Phenomena in Ultra-fine Environments* (Nauka, Moscow, 1984), In Russian.

[2] R. Birringer and H. Gleiter, In: *Encyclopedia of Materials. Sci. and Eng. Suppl.1*, ed. R.W.Cahn (Pergamon Press, 1988) p.339.

[3] A.A. Nazarov and R.R.Mulyukov, In: *Handbook of Nanoscience, Engineering, and Technology*, ed. by W. Goddard, D. Brenner, S. Lyshevski and G. Iafrate (CRC Press, 2002) p.22-1.

[4] R.Z.Bakhtizin, V.M.Lobanov and Yu.M.Yumaguzin // *Apparatus and technique of experiments* **4 (**1987) 247, In Russian.

[5] P.A.Anderson // *Phys.Rev.* **88** (1952) 655.

[6] R.R. Mulyukov and Yu.M. Yumaguzin // *Doklady Phys.* **399** (2004) 730.

[7] N.I. Noskova, E.G. Volkova, R.R. Mulyukov, A.V. Korznikov, L.R. Zubairov, In: *Proc. of Int. Conf. 'Current Status of Theory and Practice of Superplasticity in Materials'* (Sci.For., 2000) p.167.

[8] R.R.Mulyukov, Yu.M. Yumaguzin, V.A. Ivchenko, L.R.Zubairov and E.A.Litvinov // *JETP Lett.* **72** (2000) 257.

[9] R.R.Mulyukov, E.A.Litvinov, L.R.Zubairov, Yu. M.Yumaguzin and V.A. Ivchenko // *Physica B* **324** (2002) 329.

[10] A. Modinos, *Field, Thermionic, and Secondary Electron Emission Spectroscopy* (Salford: University of Salford, Plenum Press, 1984).

[11] R.Z. Valiev, A.V. Korznikov and R.R. Mulyukov // *Mater.Sci.Eng.* **A168** (1993) 141.

[12] R.Z. Valiev, R.R. Mulyukov and V.V. Ovchinnikov // *Phil.Mag.Let.* **62** (1990) 253.

[13] R.Z. Valiev, R.R. Mulyukov, V.V. Ovchinnikov and V.A. Shabashov // *Scr. Met. et Mat.* **25** (1991) 2717.

[14] N.I.Noskova and R.R.Mulyukov, *Submicrocrystalline and nanocrystalline metals and alloys* (Ekaterinburg: UB RAS, 2003), In Russian.

[15] E.A. Litvinov, L.R. R.R. Mulyukov, Zubairov, Yu. M.Yumaguzin and V.A.Ivchenko // *Tech.Phys.* **74** (2004) 96.

[16] M.I. Elinson and G.F. Vasiljev, *Autoelectron emission* (Nauka: Moscow, 1958), In Russian.

[17] L.N. Dobretsov and M.V. Gomoyumova, Emission electronics (Nauka: Moscow, 1966), In Russian.